Electronic Supplementary Information

Methods

The crystalline phases and morphology of the COFs were characterized by powder X-ray diffraction (PXRD Rigaku MiniFlex 600), scanning electron microscopy (SEM, Nova Nano 230), transmission electron microscopy (TEM, FEI TECNAI G2F20). Structural information was obtained employing Fourier transform infrared (FTIR, Thermo Nicolet Magna 670), solid-state ^{13}C cross polarization-magic angle spinning nuclear magnetic resonance (^{13}C CP/MAS ssNMR, Bruker Advance III 500) as well as X-ray photoelectron spectroscopy (XPS, Thermo ESCALAB250). Elemental analysis (EA) was conducted on Elementary Vario MICRO cube. The porosity of the photocatalysts was assessed by nitrogen sorption isotherms at 77 K after degassing, which is conducted on Micromeritics ASAP 2460. Absorption spectra were recorded on a PerkinElmer Lambda UV-vis spectrophotometer. Temperature-dependent photoluminescence (PL) and fluorescence lifetimes of samples were estimated on a FS/FL920 time-resolved fluorescence spectrometer. Electron paramagnetic resonance (EPR) measurements were performed on Bruker model A300 spectrometer and photoelectrochemical properties of the samples were studied on a BioLogic VSP-300 electrochemical system.

Materials

o-Dichlorobenzene (*o*-DCB), and *n*-butanol (*n*-BuOH) were purchased from Sinopharm Chemical Reagent Co., Ltd, Shanghai, China. Tris(4-aminophenyl)benzene, myristyltrimethylammonium bromide, and benzoyl peroxide (75%, ca 25% water content) were purchased from Beijing InnoChem Science & Technology Co., Ltd, Beijing, China. 1,3,5-Trioxane, and hydrobromic acid (47%) were purchased from TCI, Shanghai, China.

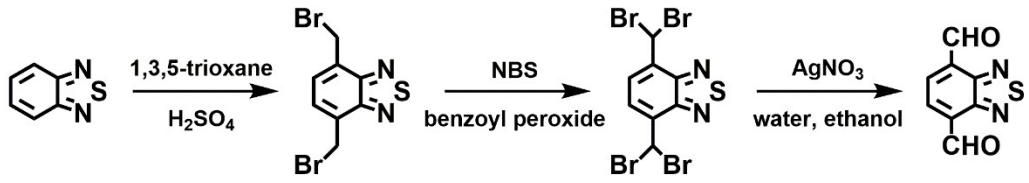

Synthesis of benzo[*c*][1,2,5]thiadiazole-4,7-dicarbaldehyde was performed using a previously reported procedure[1].

4,7-Bis(bromomethyl)benzo[*c*][1,2,5]thiadiazole (1). To the stirred solution of 2,1,3-benzothiadiazole (3.0 g, 22.01 mmol) in 48% aqueous hydrobromic acid (HBr, 60 mL) and sulfuric acid (15 mL) were added 1,3,5-trioxane (10.0 g, 111 mmol) and myristyltrimethylammonium bromide (0.75 g, 2.2 mmol). The solution was heated to reflux for 16 h. After cooling to room temperature, the reaction mixture was poured into an ice/water mixture, filtered, and washed with water. The solids were then dried under vacuum to afford the compound as a white solid. Yield: (6.6 g, 93%). ^{1}H NMR ($CDCl_3$, 500 MHz) δ (ppm) = 7.63 (s, 2 H), 4.97 (d, 4 H).

Benzo[*c*][1,2,5]thiadiazole-4,7-dicarbaldehyde (3). To a mixture of compound **1** (3.0 g, 9.0 mmol) and *N*-bromosuccinimide (NBS) (4.4 g, 37.3 mmol) in tetrachloromethane (30 mL) was added benzoyl peroxide (70 mg, 0.3 mmol). The mixture was heated under reflux for 24 h. The reaction mixture was cooled to room temperature. Afterward, the mixture was filtered and then dried under vacuum to give an off-white solid **2**. ^{1}H NMR ($CDCl_3$, 500 MHz), δ (ppm) = 8.12 (2H, s), 7.44 (2H, s). Compound **2** was then used without further purification.

A solution of the compound **2** (4 g, 16.8 mmol) in ethanol (100 mL) was heated to reflux. To this a solution of silver nitrate (6.0 g, 35.3 mmol) in 5 mL water was added. The mixture was kept under reflux for 24 h. The reaction mixture was then cooled to room temperature. The solids were filtered off and washed with water and ethanol. The filtrate was collected, and solvents were removed by rotary evaporation to give the yellow solid. The residue was purified with silica gel column chromatography and washed with dichloromethane to give compound BT as pale-yellow solid. Yield: (420 mg, 52%).^{1}H NMR ($CDCl_3$, 500

MHz) δ (ppm) = 10.93 (2H, s), 8.36 (2H, s).

N_0-COF. Tris(4-aminophenyl)benzene (20 mg, 0.057 mmol), benzo[c][1,2,5]thiadiazole-4,7dicarbaldehyde (15.6 mg, 0.081 mmol) and o-DCB/n-BuOH (1:1 in vol, 1 mL) were added to a 10 mL Pyrex tube. After ultrasonication for 1 min, 0.1 mL of acetic acid (6 M) was added. After the mixture was ultrasonicated for a further 1 min, the tube was flash frozen at 77 K using a liquid N_2 bath and degassed by three freeze-pump-thaw cycles, sealed under vacuum, and then heated at 120 °C for 3 days. A deep orange-red precipitate was formed, which was collected by suction filtration and washed with N,N'-dimethylformamide (10 mL), and acetone (10 mL) three times. The collected sample was dried under vacuum for 24 h to give an orange-red powder (30 mg, 92%). Elemental analysis (%): Anal. Calcd. For ($C_{72}H_{54}N_{12}S_3$, theoretical formula for an infinite 2D COF): C, 73.83; N, 14.35. Found: C, 71.80; N, 13.70.

N_3-COF. Tris(4-aminophenyl)benzene (20 mg, 0.057 mmol), benzo[c][1,2,5]thiadiazole-4,7dicarbaldehyde (15.6 mg, 0.081 mmol) and o-DCB/n-BuOH (1:1 in vol., 1 mL) were added to a 10 mL Pyrex tube. After ultrasonication for 1 min, 0.1 mL of acetic acid (6 M) was added. After the mixture was ultrasonicated for a further 1 min, the tube was flash-frozen at 77 K using a liquid N_2 bath and degassed by three freeze-pump-thaw cycles, sealed under vacuum, and then heated at 120 °C for 3 days. A deep orange-red precipitate was formed, which was collected by suction filtration and washed with N,N'-dimethylformamide, (10 mL), and acetone (10 mL) three times. The collected sample was dried under vacuum for 24 h to give a deep orange powder (30 mg, 92%). Elemental analysis (%): Anal. Calcd. For ($C_{66}H_{48}N_{18}S_3$, theoretical formula for an infinite 2D COF): C, 67.28; N, 21.42. Found: C, 64.64; N, 20.33.

Photoelectrochemical measurements

Working photoelectrode is constructed by the as-prepared COF powder. Specifically, COF powder (5 mg) and Nafion (100 μL) were blended into DMF (900 μL) as stock solution. Subsequently, the as-prepared solution (10 μL) was drop-coated on a clean FTO glass, and the COF based photoelectrode can be obtained by drying the DMF in

ambient condition. Transient photocurrent response, linear sweep voltammetry (LSV), and Mott-Schottky plot of electrochemical impedance spectroscopy (EIS) were conducted by a three-electrode system, using COF-based electrode as working electrode, Pt foil (1.0 × 1.0 cm^2) as counter electrode, and Ag/AgCl as reference. Especially, the flat band potential can be obtained by plotting the tangent line of Mott-Schottky spectra. The intersection point of the tangent line and a-axis can be applied as the conduction band[2].

Photocatalytic H_2O_2 production

10 mg of COF was added to 20 mL of deionized water in a glass bottle (50 mL), and the bottle was sealed with a two-way valve that connected to an O_2 balloon. The catalyst was dispersed by ultrasonication for 5 mins and remained stirring at 900 rpm during reaction period. The bottle was kept at 30 ºC by circulating water and was irradiated by 495 nm LED monochromatic light. The distance between the light source and the bottle was 6.0 cm.

The quantity of H_2O_2 was determined by the colorimetric method. Specifically, 1 mL $Ti(SO_4)_2$ solution was added into 5.0 mL of reaction solution containing produced H_2O_2. Then the mixed solution was transferred into a vessel and determined by UV–Vis spectrophotometer.

$Ti(SO_4)_2$ solution was prepared as an indicator to interact with H_2O_2. In detail, 1g TiO_2 was blended in100 mL H_2SO_4 solution (98%), and thermally treated at 155 °C for 20 h under stirring. The $Ti(SO_4)_2$ reaction solution can be collected by filtering off the undissolved TiO_2 powder. The Ti^{4+} abundant solution will become a yellow complex when it interacts with H_2O_2 as shown in Equation S1[3].

$$Ti(SO_4)_2 + H_2O_2 \rightarrow H_2[Ti_2(SO_4)_2] \qquad \text{Equation (S1)}$$

Calibrations for the measurements of the H_2O_2 solution. H_2O_2 solution with the concentration of 0.5, 1, 1.5, 2.5, 5 mmol/L were prepared. The as-prepared solution (5 mL) was added into the $Ti(SO_4)_2$ solution, and monitored by UV–Vis spectrophotometer. The calibration curve is presented in Fig. S22, and linear fitting of the calibration indicates the measurement of H_2O_2 concentration is accurate with this approach.

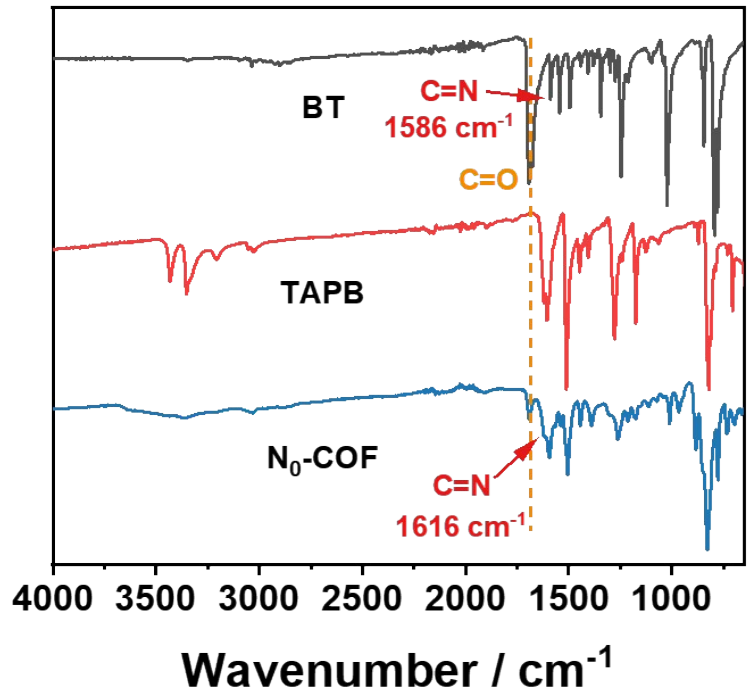

Fig. S1 FT-IR spectra of N_0-COF and BT/TAPB monomers.

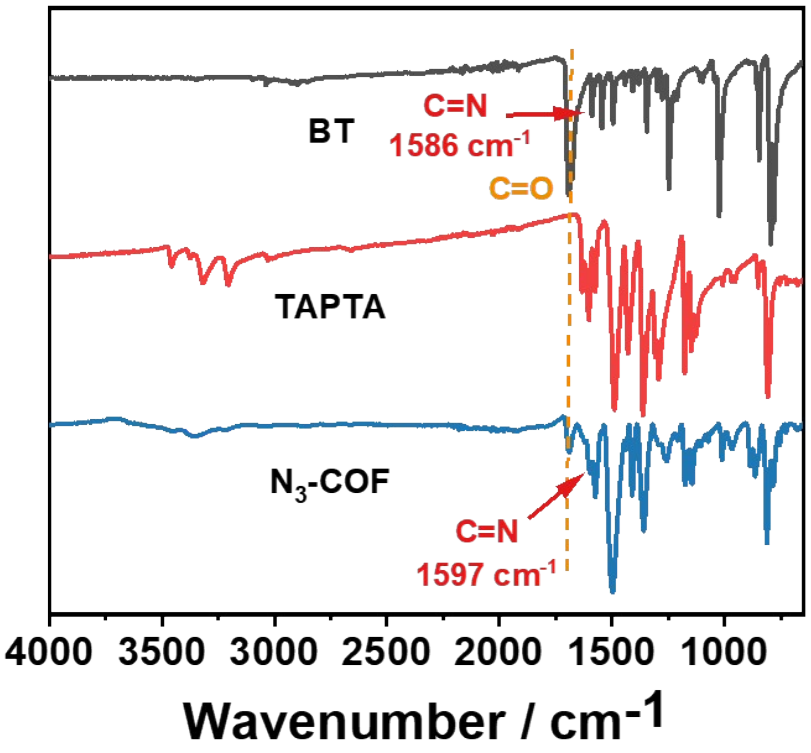

Fig. S2 FT-IR spectra of N_3-COF and BT/TAPA monomers.

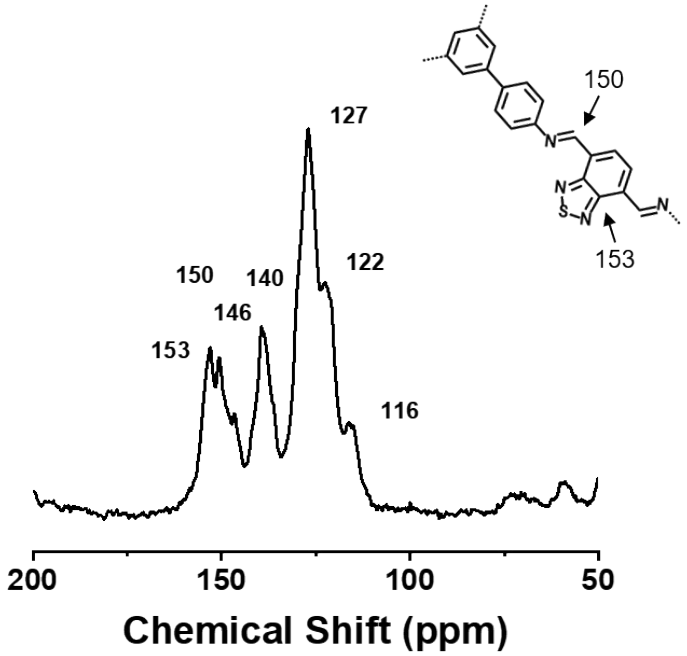

Fig. S3 ^{13}C CP/MAS solid-state NMR spectrum of N_0-COF.

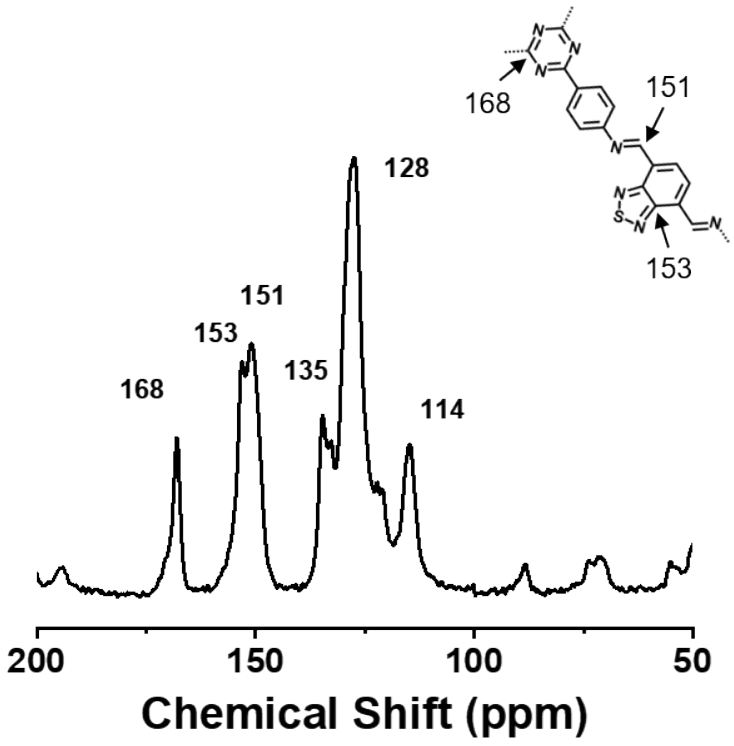

Fig. S4 ^{13}C CP/MAS solid-state NMR spectrum of N_3-COF.

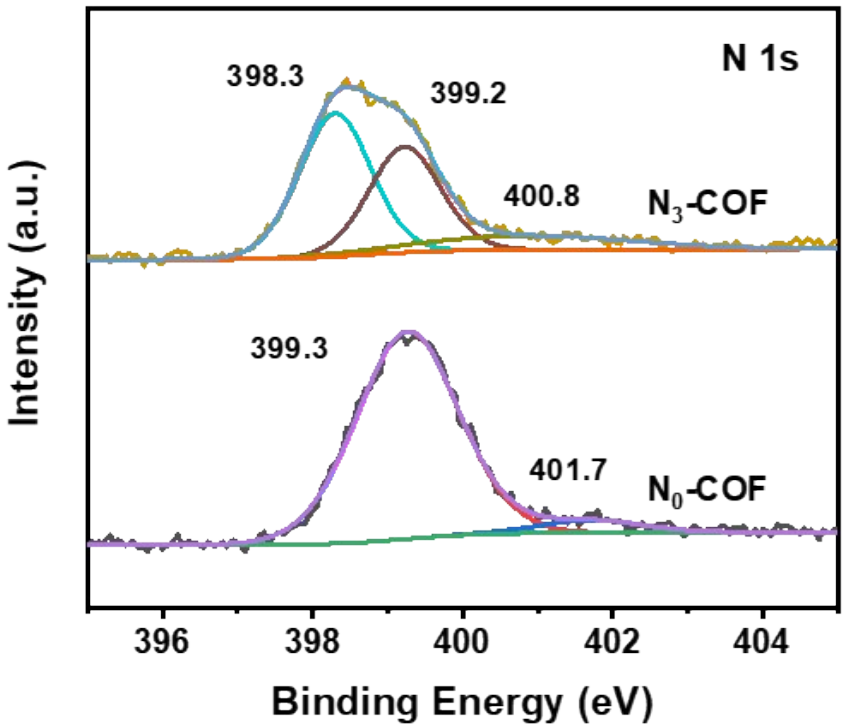

Fig. S5 N 1s XPS spectra of N_3-COF and N_0-COF.

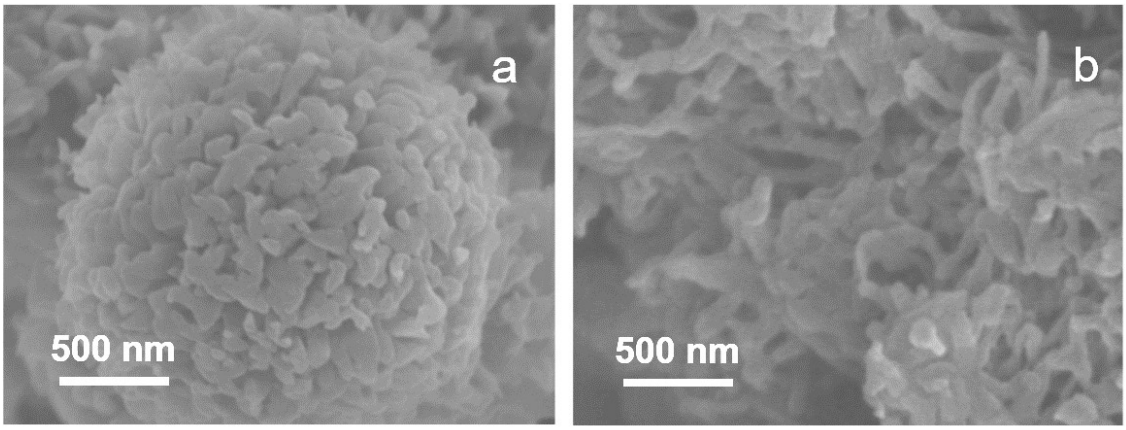

Fig. S6 SEM images of (a) N_0-COF and (b)N_3-COF.

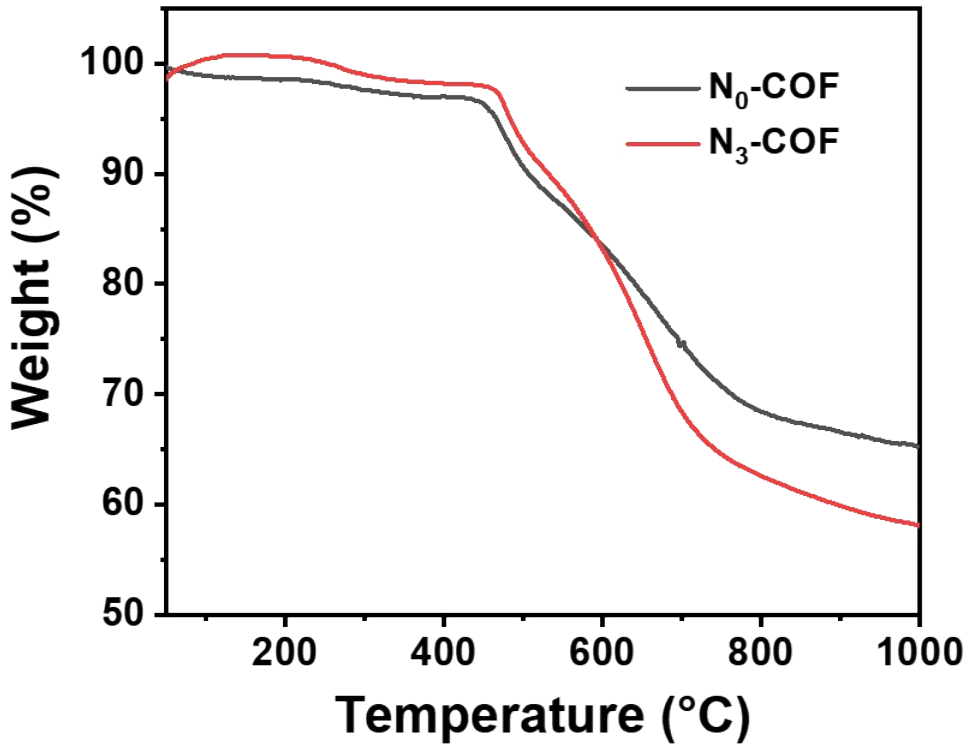

Fig. S7 TGA profiles of N_3-COF and N_0-COF.

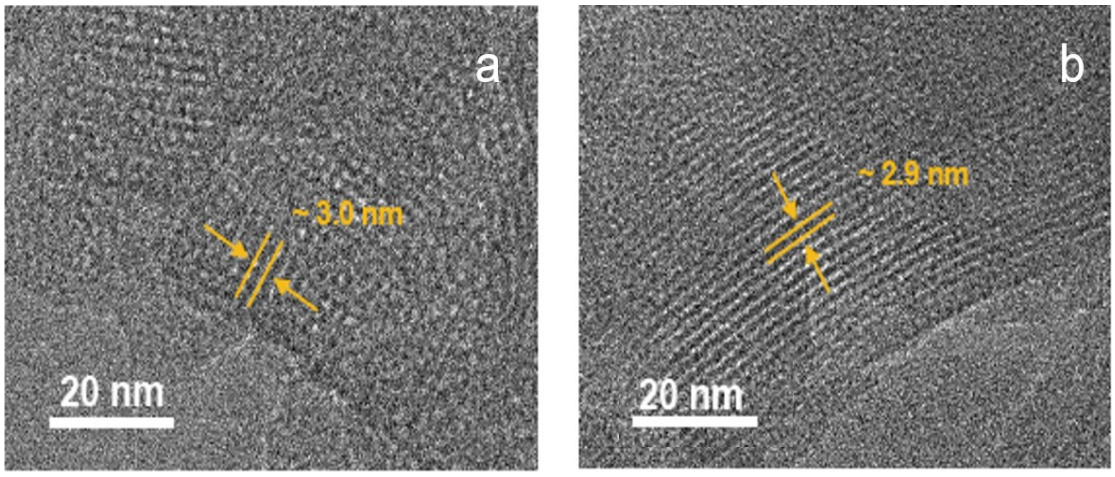

Fig. S8 HR-TEM images of (a) N_0-COF and (b) N_3-COF.

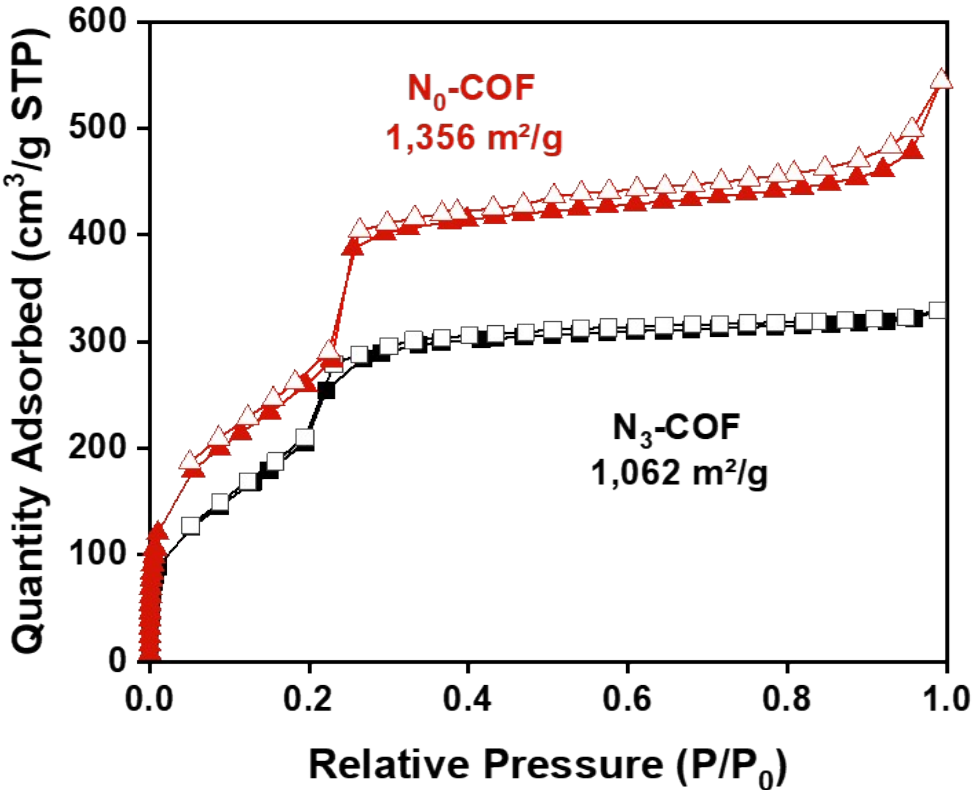

Fig. S9 N_2 sorption isotherms at 77 K for N_0-COF (red) and N_3-COF (black).

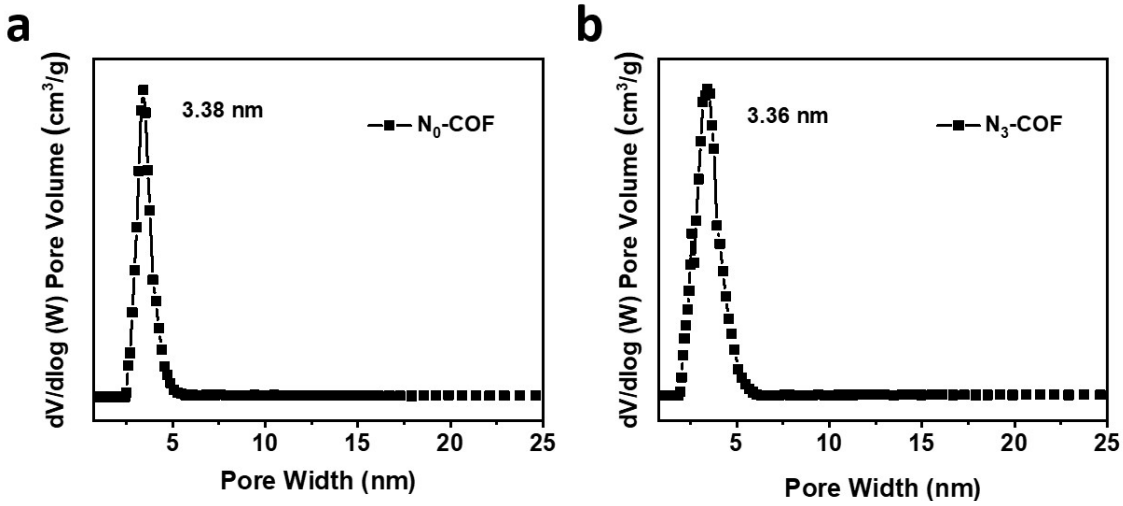

Fig. S10 The pore size distribution profiles of (a) N_0-COF and (b) N_3-COF.

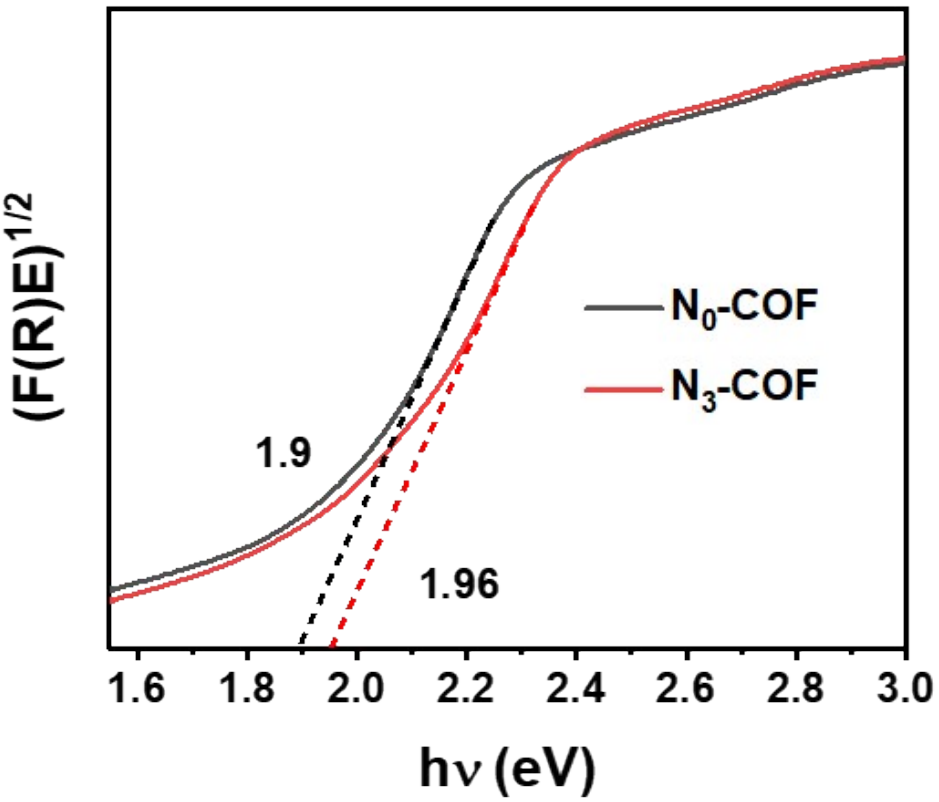

Fig. S11 Kubelka-Munk plots of N_0-COF and N_3-COF.

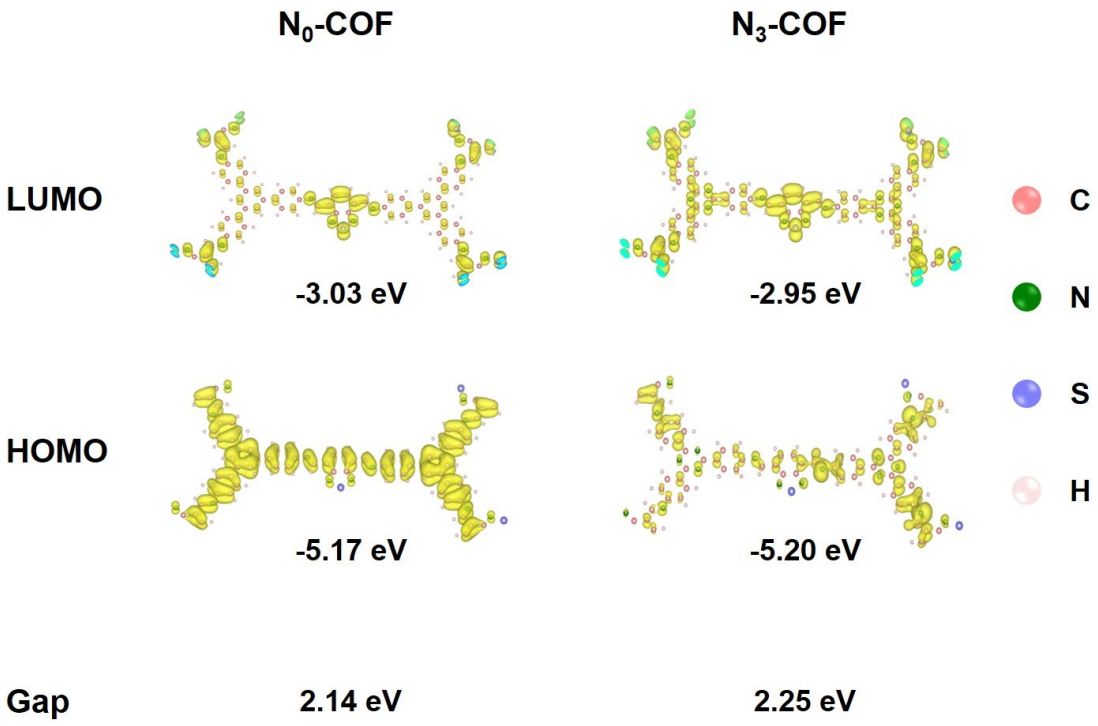

Fig. S12 HOMO and LUMO diagrams of N_3-COF and N_0-COF.

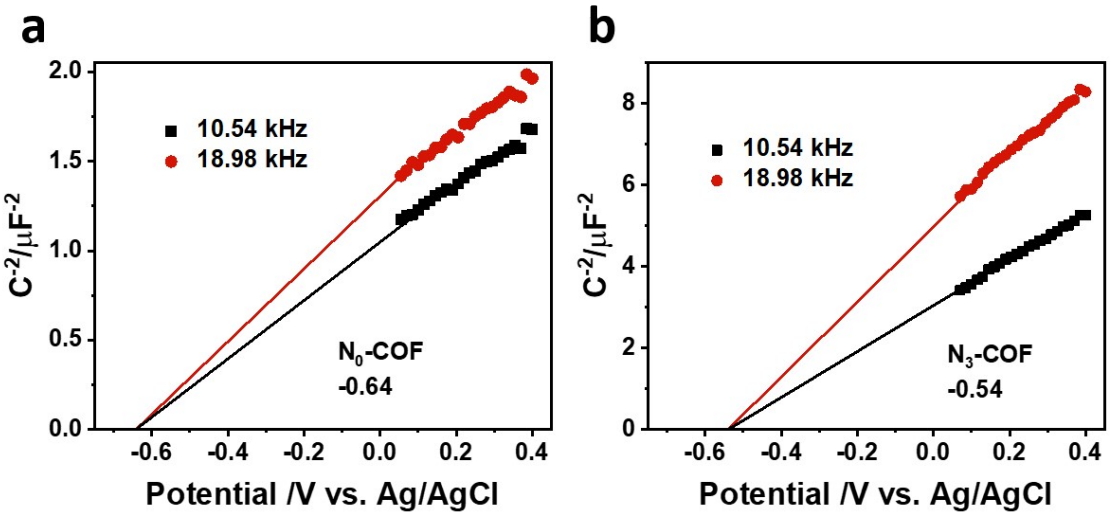

Fig. S13 Mott-Schottky plots of (a) N_0-COF and (b) N_3-COF.

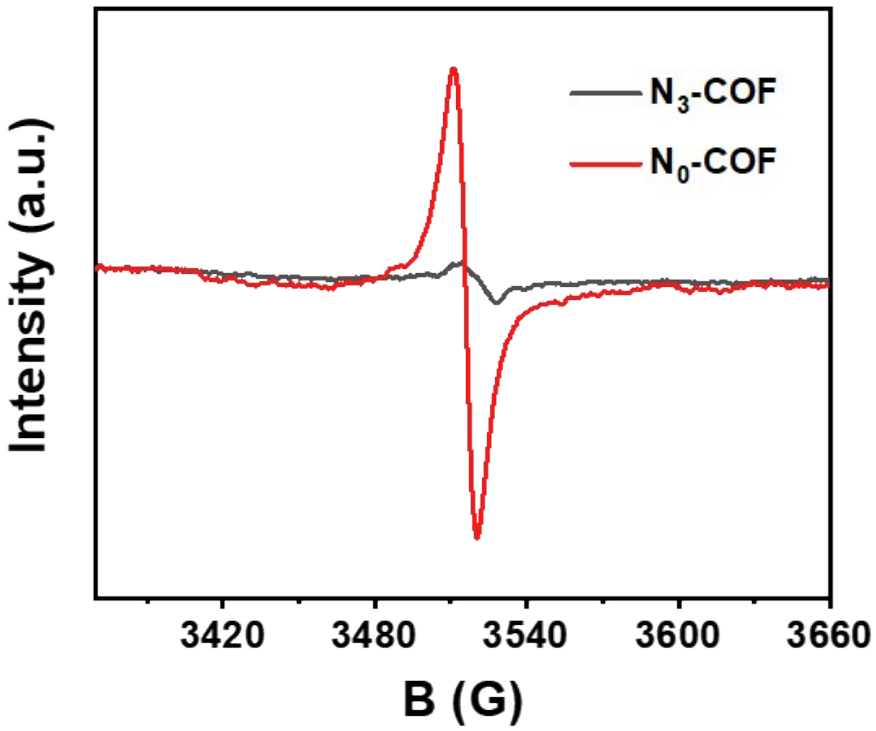

Fig. S14 EPR spectra of N_0-COF (red) and N_3-COF (black) (irradiation light source: 300 W Xe lamp).

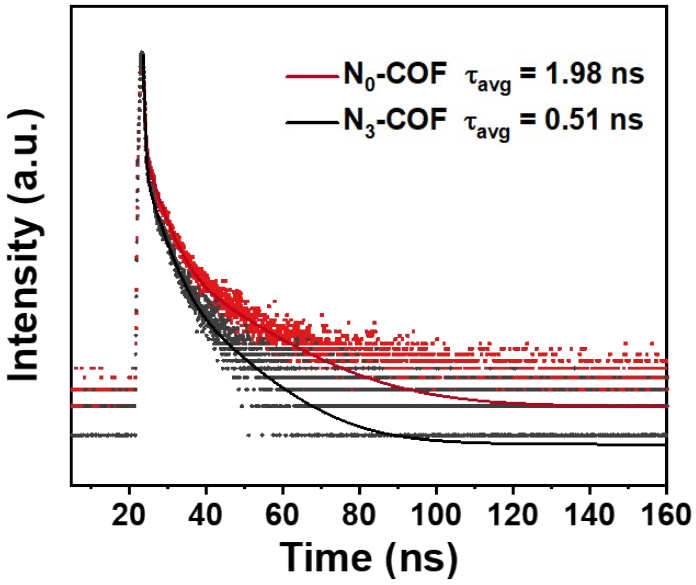

Fig. S15 Time-resolved photoluminescence spectra of N_0-COF and N_3-COF.

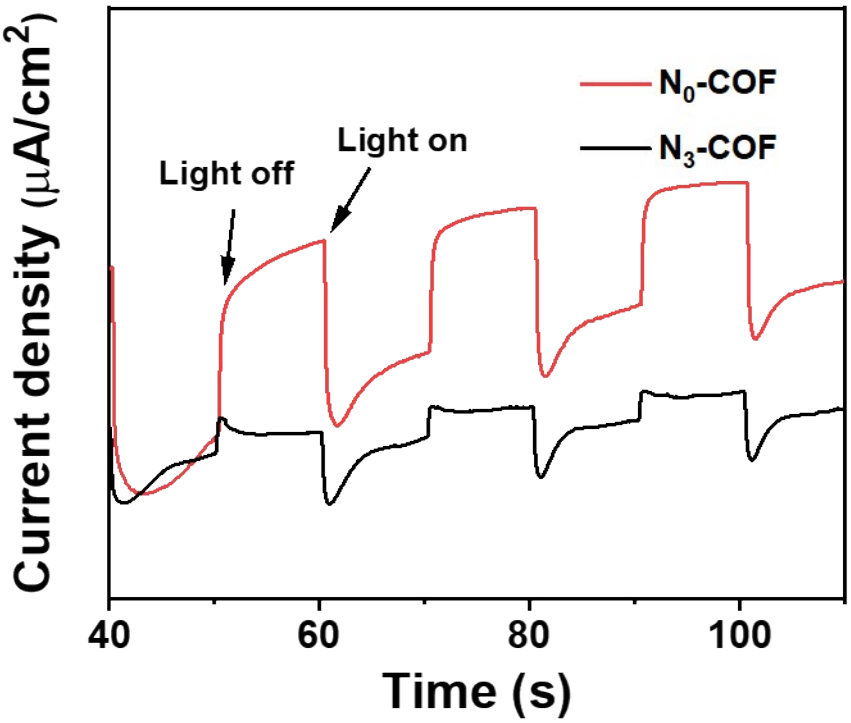

Fig. S16 Transient photocurrent responses of N_0-COF (red) and N_3-COF (black).

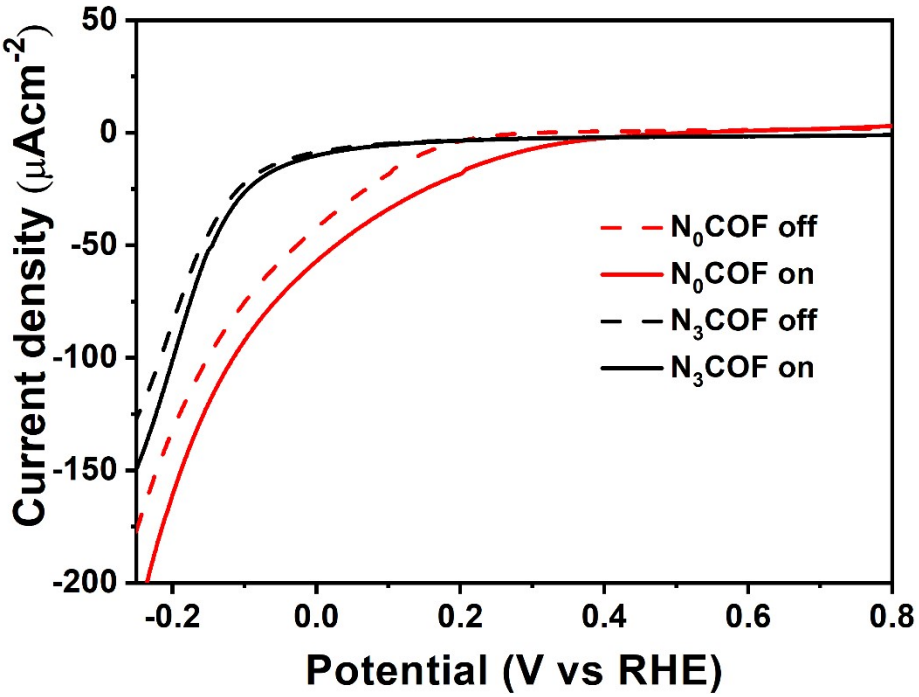

Figure S17 The LSV diagrams of N_0-COF and N_3-COF.

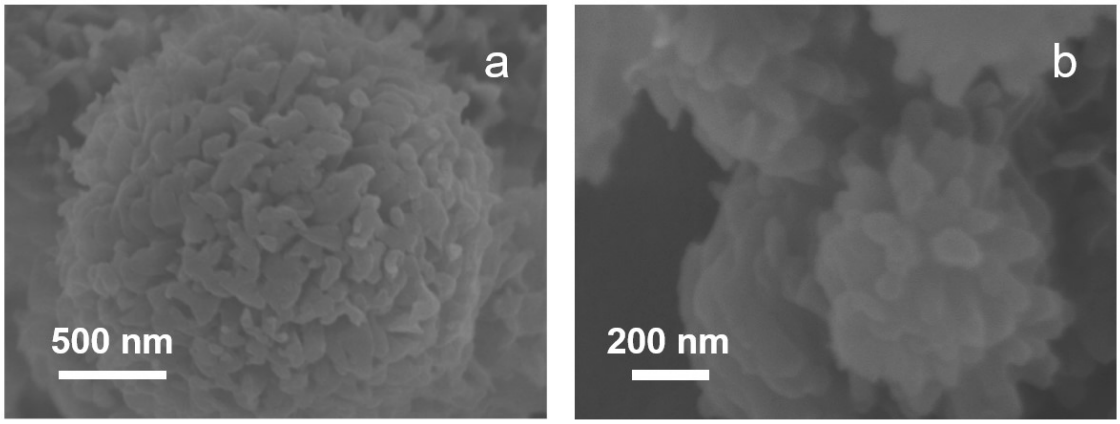

Fig. S18 SEM images of N_0-COF before (a) and after (b) the H_2O_2 production reaction.

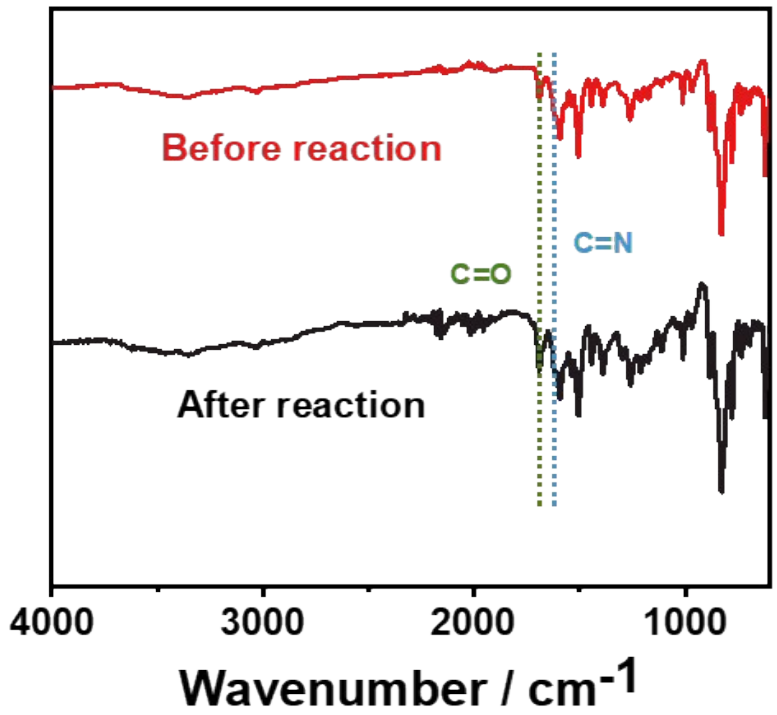

Fig. S19 FT-IR spectra of N_0-COF before and after the reaction.

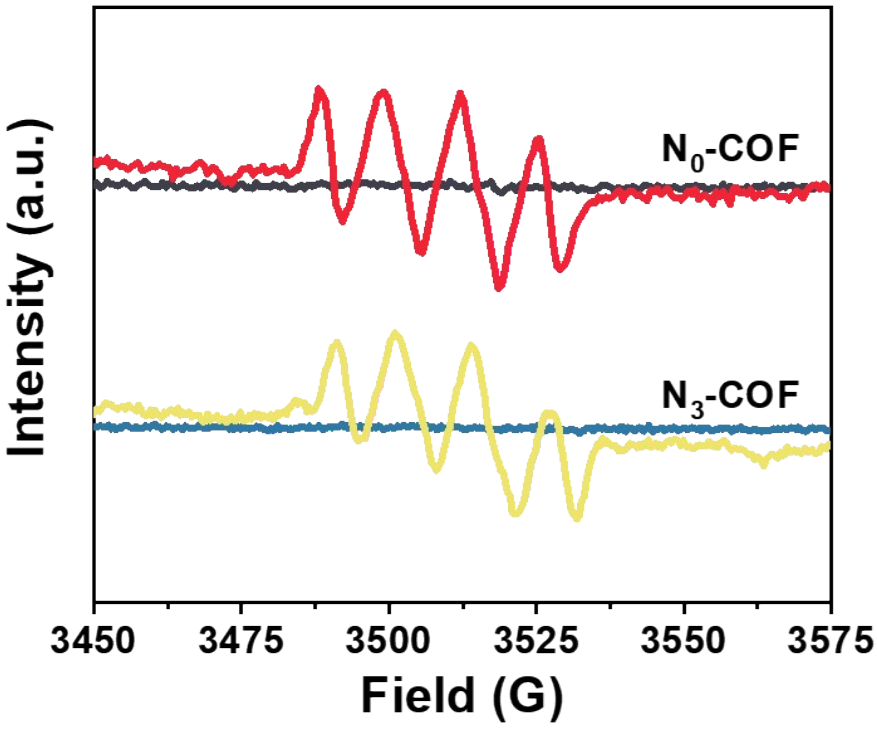

Fig. S20 EPR spectra of DMPO adduct measured in the solution of methanol for N_0-COF (red) and N_3-COF (yellow) exposed to visible light and N_0-COF (black) and N_3-COF (blue) in the dark.

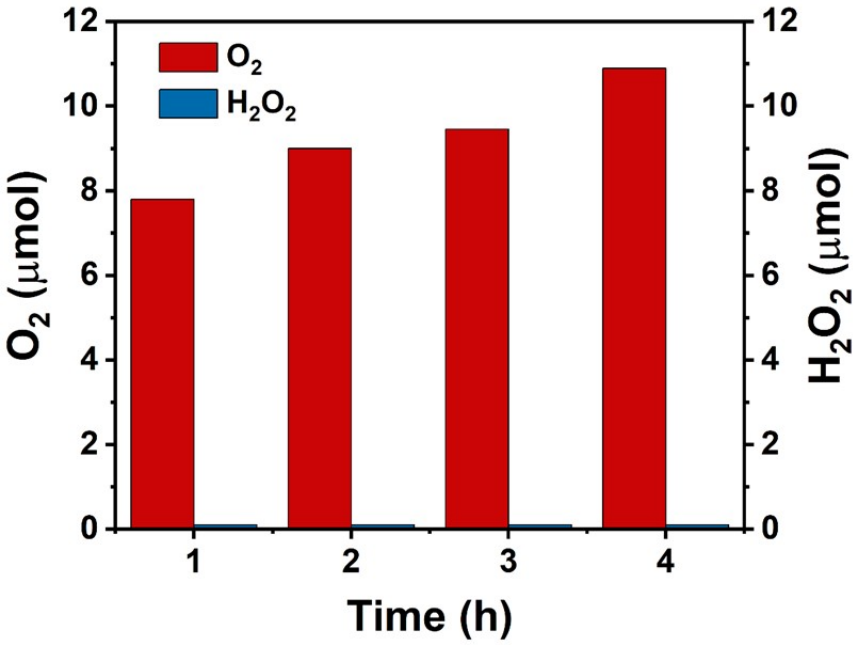

Fig. S21 The production of O_2 of N_0-COF via water oxidation half-reaction (reaction condition: 20 mg catalyst, 100 mL water, 0.2 g La_2O_3, 0.17 g $AgNO_3$, 120 μL $CoNO_3$ water solution, $\lambda > 300$nm).

Note: The water oxidation reaction took place by using N_0-COF as the photocatalyst, and the O_2 yield was about 7.8 μmol at the first hour. However, with prolonged reaction times, the oxygen evolution rate gradually decreased, which may be caused by the deposition of Ag nanoparticles on the surface of the COF catalyst (formed during the photoreduction of Ag^+), which results in a light shading effect and hinders optical absorption[4].

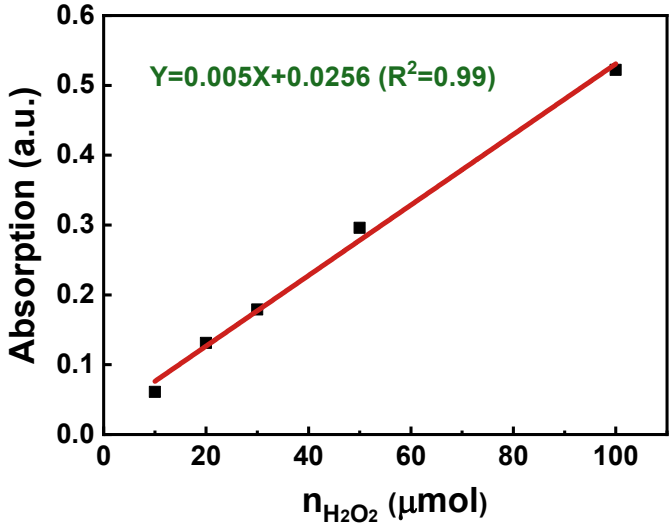

Fig. S22 Calibration for the H_2O_2 measurement.

Table S1 Elemental analysis of N_0-COF and N_3-COF.

Sample		N [%]	C [%]	H [%]	C/N molar ratio
N_0-COF	Found	13.70	71.80	3.82	5.24
	Anal. Calcd	14.35	73.83	3.61	5.14
N_3-COF	Found	20.33	64.64	3.14	3.18
	Anal. Calcd	21.42	67.28	3.08	2.95

Table S2 The comparison of photocatalytic performance for N_0-COF and other reported photocatalysts.

Photocatalytic system	The amounts of photocatalyst	Irradiation condition	H_2O_2 production rate (μmol h^{-1})	Sacrificial agent	Ref.
g-C_3N_4/PDI/r$GO_{0.05}$	50 mg	λ>420 nm 2 kW Xe lamp	1.2	No	5
P-C_3N_4 with heteroatom S and K doping (Flux growth method) AKMT	1 mg	λ>420 nm 300 W Xe lamp	175	Ethanol	6
Graphene oxide	320 mg	Simulation sunlight 765 W Xe lamp	50	No	7
Si/TiO_2-Au	Fiber	λ=365 nm	38	No	8
Ni/MIL-125-NH_2	5 mg	λ>420 nm 500 W Xe lamp	7	TEOA	9
PCN-OH	40 mg	λ>400 nm 300 W Xe lamp	728	Ethanol	10
TAPD-$(Me)_2$ COF	20 mg	λ=400-700 nm	4.6	Ethanol	11

Au-TiO_2	200 mg	λ>300 nm high-pressure mercury lamp	300	Ethanol	12
Sb single atom photocatalyst (Sb-SAPC15)	100 mg	λ>420 nm 500 W Xe lamp	180	No	13
covalent heptazine frameworks with diphenyldiacetylene (CHF-DPDA)	40 mg	λ>420 nm 300 W Xe lamp	69	No	14
TTA-TTTA-COF	15 mg	λ=420 nm LED lamp	36	No	15
N_0-COF	**10 mg**	**λ=495 nm LED lamp**	**15.7**	**No**	**This work**

Table S3 Control experiments of reaction mechanism exploration for N_0-COF

Entry	Photocatalyst	Solvent system	Gas	Irradiation conditions	H_2O_2 produced (μmol h^{-1})
1	Blank	Water	O_2	λ=495 nm	0
2	N_0-COF	Water	O_2	Dark	0
3	N_0-COF	Water	Ar	λ=495 nm	0
4	N_0-COF	Water	Benzoquinone: Radical scavenger	λ=495 nm	0
5	N_0-COF	Water	O_2	λ=495 nm	15.7

Table S4 Reaction seats of N_0-COF.

N_0-COF	Front view	Top view
Far from C3 axis	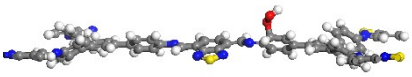	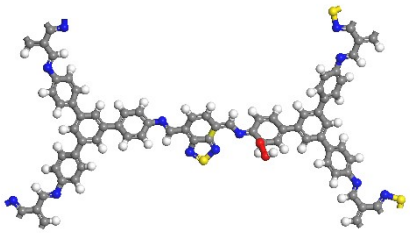
Between C and N	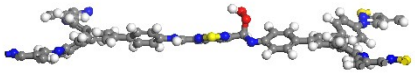	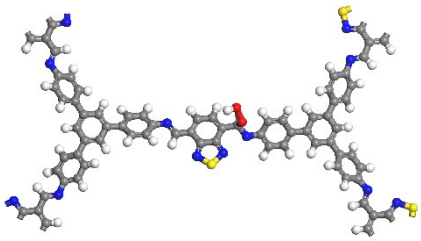
Near C3 axis	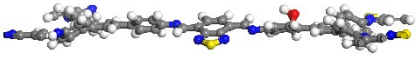	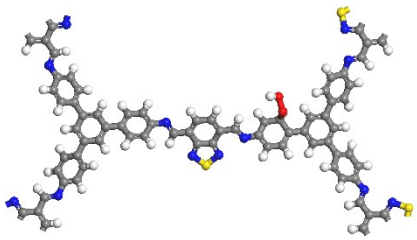
Near S atom	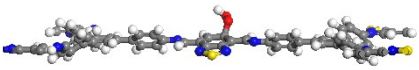	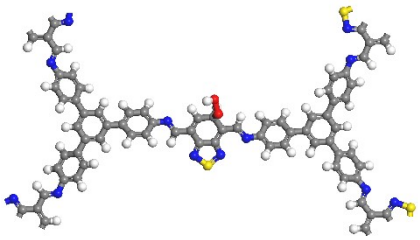

Table S5 Reaction seats of N_3-COF.

N_3-COF	Front view	Top view
Far from C3 axis	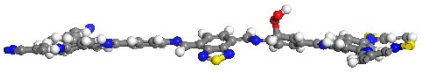	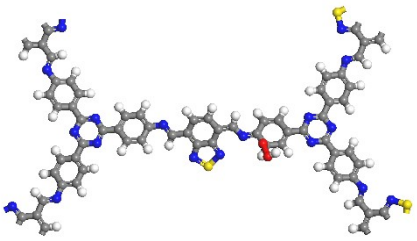
Between C and N	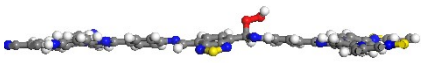	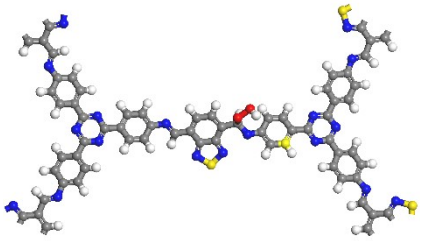
Near C3 axis	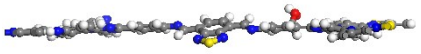	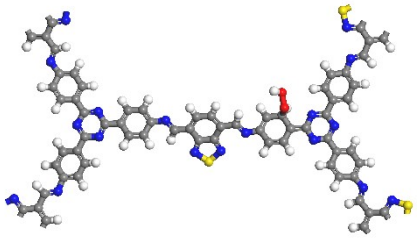
Near S atom	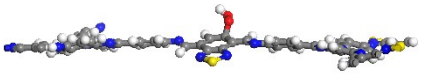	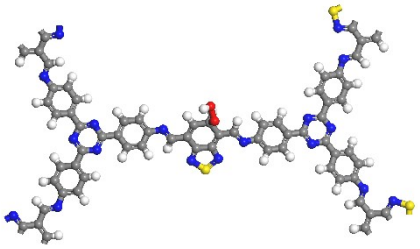

Supplementary references

1. W. Chen, Z. Yang, Z. Xie, Y. Li, X. Yu, F. Lu and L. Chen, *J. Mater. Chem. A*, 2019, **7**, 998-1004.
2. W.-J. Chun, A. Ishikawa, H. Fujisawa, T. Takata, J. N. Kondo, M. Hara, M. Kawai, Y. Matsumoto and K. Domen, *J. Phys. Chem. B*, 2002, **107**, 1798–1803.
3. X. Chen, J. Zhang, X. Fu, M. Antonietti and X. Wang, *J. Am. Chem. Soc.*, 2009, **131**, 11658–11659.
4. Z.-A. Lan, Y. Fang, Y. Zhang and X. Wang, *Angew. Chem. Int. Ed.*, 2018, **57**, 470-474.
5. Y. Kofuji, Y. Isobe, Y. Shiraishi, H. Sakamoto, S. Tanaka, S. Ichikawa and T. Hirai, *J. Am. Chem. Soc.*, 2016, **138**, 10019-10025.
6. P. Zhang, Y. Tong, Y. Liu, J. J. M. Vequizo, H. Sun, C. Yang, A. Yamakata, F. Fan, W. Lin, X. Wang and W. Choi, *Angew. Chem. Int. Ed.*, 2020, **59**, 16209-16217.
7. W.-C. Hou and Y.-S. Wang, *ACS Sustainable Chem. Eng.*, 2017, **5**, 2994-3001.
8. N. Kaynan, B. A. Berke, O. Hazut and R. Yerushalmi, *J. Mater. Chem. A*, 2014, **2**, 13822-13826.
9. Y. Isaka, Y. Kondo, Y. Kawase, Y. Kuwahara, K. Mori and H. Yamashita, *Chem. Commun.*, 2018, **54**, 9270-9273.
10. W. Hou, Y. Li, S. Ouyang, H. Chen, J. Ye, X. Han and Y. Deng, *Chem. Commun.*, 2019, **55**, 13279-13282.
11. C. Krishnaraj, H. Sekhar Jena, L. Bourda, A. Laemont, P. Pachfule, J. Roeser, C. V. Chandran, S. Borgmans, S. M. J. Rogge, K. Leus, C. V. Stevens, J. A. Martens, V. Van Speybroeck, E. Breynaert, A. Thomas and P. Van Der Voort, *J. Am. Chem. Soc.*, 2020, **142**, 20107-20116.
12. M. Miwako Teranishi, S.-i. Naya and H. Tada, *J. Am. Chem. Soc.*, 2010, **132**, 7850–7851.
13. Z. Teng, Q. Zhang, H. Yang, K. Kato, W. Yang, Y.-R. Lu, S. Liu, C. Wang, A. Yamakata, C. Su, B. Liu and T. Ohno, *Nat. Catal.*, 2021, **4**, 374-384.
14. H. Cheng, H. Lv, J. Cheng, L. Wang, X. Wu and H. Xu, *Adv. Mater.*, 2021, **2107480**
15. F. Tan, Y. Zheng, Z. Zhou, H. Wang, X. Dong, J. Yang, Z. Ou, H. Qi, W. Liu, Z. Zheng and X. Chen, *CCS Chem.*, 2022, DOI: 10.31635/ccschem.022.202101578.